Eur. Phys. J. Appl. Phys. **45**, 31101 (2009)
DOI: 10.1051/epjap/2009012

THE EUROPEAN PHYSICAL JOURNAL APPLIED PHYSICS

An analytical model for the ΔE effect in magnetic materials

L. Daniel[1,a] and O. Hubert[2]

[1] LGEP, CNRS-UMR 8507, Supélec, Univ. Paris-Sud, UPMC Paris 6, Plateau de Moulon, 11 rue Joliot-Curie, 91192 Gif-sur-Yvette Cedex, France
[2] LMT-Cachan – ENS Cachan, CNRS-UMR 8535, UPMC Paris 6, 61 avenue du Président Wilson, 94235 Cachan Cedex, France

Received: 23 November 2007 / Received in final form: 16 December 2008 / Accepted: 22 December 2008
Published online: 6 February 2009 –

Abstract. The ΔE effect is often presented as the dependency of the Young's modulus of a material on its state of magnetization. Nevertheless, the elastic properties of a magnetic material do not depend on the magnetization state. Actually, the sensitivity of the magnetostriction strain to the application of a stress explains the ΔE effect. According to this statement, a semi-analytical model for the ΔE effect is proposed, in which magnetization rotation is not considered. An experimental procedure to measure the ΔE effect in magnetic materials is then built-up. Experimental and modeling results are finally compared, with satisfying agreement.

PACS. 75.80.+q Magnetomechanical and magnetoelectric effects, magnetostriction – 46.25.Hf Thermoelasticity and electromagnetic elasticity

1 Introduction

The Young's modulus E of a material is the ratio between the stress σ and the elastic strain ε^{el} – measured in the direction parallel to the applied stress – in the case of a tension or compression test (Eq. (1))

$$E = \frac{\sigma}{\varepsilon^{el}}. \tag{1}$$

When a stress is applied to a magnetic material, stress-strain response appears to be non-linear (Fig. 1). This effect is called the ΔE effect [1,2]. It is often presented as a dependency of the Young's modulus E to the stress level. On the other hand, the ΔE effect depends on the state of magnetization of the material as illustrated in Figure 1: the Young's modulus of a demagnetized specimen appears to be lower than the Young's modulus of the same specimen magnetized at saturation. Thus, the ΔE effect could be seen as an apparent loss of linearity in the elastic behavior of demagnetized specimens. But it can also be interpreted as a consequence of the effect of stress on the magnetostriction strain (magnetostriction is the spontaneous deformation associated to magnetic domain structure evolution). The ΔE effect can consequently be dissociated from the elastic behavior.

Indeed, the application of stress modifies the magnetization state of magnetic materials and generates a magnetostriction strain. This magnetostriction strain ε^{μ} is superimposed to the elastic strain ε^{el}, so that the total measured strain ε is defined by equation (2), all the strains being measured in the direction parallel to the applied stress

$$\varepsilon = \varepsilon^{\mu} + \varepsilon^{el}. \tag{2}$$

The apparent Young's modulus E_a is defined by equation (3)

$$E_a = \frac{\sigma}{\varepsilon^{\mu} + \varepsilon^{el}}. \tag{3}$$

In the case of a saturated material, the magnetic domain structure has reached a saturated configuration and the magnetostriction strain cannot evolve anymore. The apparent Young's modulus E_a^s is then defined by equation (4), corresponding to the original definition of the

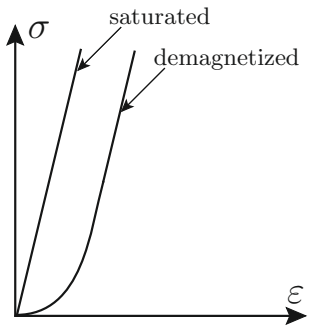

Fig. 1. Illustration of ΔE effect on a tensile stress-strain curve (ε is the total strain).

[a] e-mail: laurent.daniel@lgep.supelec.fr

Young's modulus given by equation (1)

$$E_a^s = \frac{\sigma}{\varepsilon^{el}} = E. \tag{4}$$

For a given initial magnetic configuration, the ΔE effect can be quantitatively defined as a function of the applied stress σ following equation (5):

$$\frac{\Delta E}{E} = \frac{E - E_a(\sigma)}{E_a(\sigma)} = \frac{\varepsilon^{\mu}(\sigma)}{\varepsilon^{el}(\sigma)}. \tag{5}$$

The value of the Young's modulus E can be easily identified thanks to an usual tensile test[1], for a stress level such that the stress-strain curve is linear. In the linearity area of the curve, we define:

$$E = \frac{d\sigma}{d\varepsilon}. \tag{6}$$

A predictive model for the ΔE effect should then rely on the description of the effect of stress on the magnetostriction strain. Very few models are available in the literature. Squire treated the case of amorphous ribbons [3], but did not address the case of crystalline materials. This latter point is the purpose of that paper. After a brief presentation of the energetic terms involved in the magnetic equilibrium of a ferro- or ferri-magnetic body volume element, a simplified approach for the ΔE effect in cubic single crystals is presented, in which magnetization rotation is not considered[2]. It is applied both for materials with positive and negative anisotropy constants. An extension to the behavior of polycrystals is then proposed and results are compared to original experimental ones.

2 Magneto-elastic equilibrium

The magneto-elastic equilibrium of a ferro- or ferri-magnetic body can be seen as the result of a competition between several energetic contributions [4].

- The exchange energy W^{ex} is related to the ferromagnetic coupling effect between neighboring atoms, tending to favor an uniform magnetization in a volume element.
- The magneto-crystalline energy W^K tends to align the magnetization along particular directions, called "easy axes". These easy magnetization directions are mostly connected to crystallographic structure. In the case of iron, whose crystallographic structure is body cubic centered, the anisotropy constant K_1 is positive and magnetization is aligned along $\langle 100 \rangle$ axes (six directions[3]). In the case of Nickel, whose crystallographic structure is face cubic centered, the easy axes are the eight $\langle 111 \rangle$ directions (Fig. 2).

[1] Whatever the magnetic state of the specimen.

[2] Rotation is the mechanism considered in [3]. In that sense, our proposal is complementary to this previous one and will not apply to amorphous materials.

[3] The notation used for the crystallographic directions refers to the Miller indices.

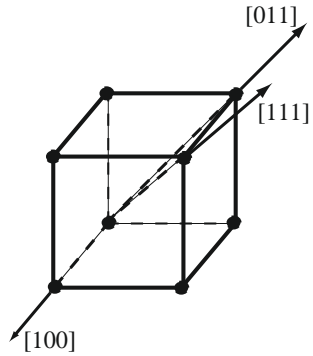

Fig. 2. Crystallographic directions in the cubic symmetry (Miller indices).

- The magneto-static energy W^{mag} tends to align the magnetization direction with the magnetic field direction, or, at least, to energetically favor domains for which the magnetization direction is close to the magnetic field direction.
- The elastic energy W^{el} introduces the magneto-elastic interactions in a ferromagnetic crystal. It is often called "magneto-elastic" energy.

The competition between these energetic contributions explains the existence of the typical magnetic domain microstructure of magnetic materials. Each magnetic domain is uniformly magnetized at saturation. For low magnetic field level, the magnetization of a magnetic domain is aligned along an easy axis.

The magnetization process is the result of two concomitant processes. On one hand, the magnetic walls, separating one domain from another, are moving, modifying the mean magnetization in the material. On the other hand, the magnetization direction can rotate out of its initial easy axis. This rotation mechanism is encountered when the energy given by the applied magnetic field is high enough to compensate the magneto-crystalline anisotropy energy. This situation is usually reached for medium to high magnetic fields. The application of a stress significantly modifies the magnetization of the material, through the contribution of the elastic energy.

Finally, the elastic energy strongly depends on the local magnetostriction strain, through the mechanical incompatibilities. This magneto-elastic coupling is at the origin of the ΔE effect.

3 A simplified approach for the ΔE effect in single crystals

We develop hereafter a simplified approach for the description of the ΔE effect in single crystals. This approach is inspired by a multiscale model for the prediction of magneto-elastic reversible behavior of ferromagnetic materials presented in [5]. The restriction to the case of no applied magnetic field allows an analytical derivation of the ΔE effect.

The approach is limited to the case when no magnetic field is applied, so that the magneto-static energy does not appear in the definition of the magnetic equilibrium ($W^{mag} = 0$).

We suppose that no rotation mechanism occurs in the magnetic domains. The magneto-crystalline anisotropy energy is then uniform within a single crystal and does not participate to the evolution of the magnetostriction strain ($W^K = \text{const.}$). The magnetization in a domain is always aligned along an easy crystallographic direction.

We choose a simplified description of the single crystal microstructure. The crystal is seen as an aggregate of magnetic domains. Considering that only easy directions can be encountered for the magnetization in the domains, we divide the single crystal into domain families (num. α), each family being associated to the corresponding easy axis. In the case of $\langle 100\rangle$ easy axes, only six domain families are possible ($\alpha = \{1, \ldots, 6\}$), eight in the case of $\langle 111\rangle$ easy axes ($\alpha = \{1, \ldots, 8\}$).

The exchange energy W^{ex} is responsible for the local coupling between magnetic moments. It does not participate anymore in the energetic description of such an aggregate (wall energy is not considered, exchange energy is hidden in the concept of domain family).

In such conditions, the elastic energy will be the only energetic term explicitly considered in the description of the magnetic equilibrium of the single crystal, because this term is not identical from one domain family to another. The elastic energy W_α^{el} of a domain α can be written [5]:

$$W_\alpha^{el} = -\boldsymbol{\sigma}_c : \boldsymbol{\varepsilon}_\alpha^\mu \tag{7}$$

where $\boldsymbol{\sigma}_c$ is the mean stress – second order – tensor within the single crystal and $\boldsymbol{\varepsilon}_\alpha^\mu$ is the magnetostriction strain – second order – tensor in the domain family α. The latter, assumed to be homogeneous within a domain family, is written, in the crystallographic coordinate system of the cubic crystal (see for instance [6]):

$$\boldsymbol{\varepsilon}_\alpha^\mu = \frac{3}{2}\begin{pmatrix} \lambda_{100}(\gamma_1^2 - \frac{1}{3}) & \lambda_{111}\gamma_1\gamma_2 & \lambda_{111}\gamma_1\gamma_3 \\ \lambda_{111}\gamma_1\gamma_2 & \lambda_{100}(\gamma_2^2 - \frac{1}{3}) & \lambda_{111}\gamma_2\gamma_3 \\ \lambda_{111}\gamma_1\gamma_3 & \lambda_{111}\gamma_2\gamma_3 & \lambda_{100}(\gamma_3^2 - \frac{1}{3}) \end{pmatrix}. \tag{8}$$

(γ_1, γ_2, γ_3) are the direction cosines of magnetization in the domain family α, λ_{100} and λ_{111} are the magnetostrictive constants of the material. If we consider a multiaxial applied stress state $\boldsymbol{\sigma}_c$, written in the crystallographic coordinate system (Eq. (9)), the elastic energy (Eq. (7)) can be written in the form of equation (10).

$$\boldsymbol{\sigma}_c = \begin{pmatrix} \sigma_{11} & \sigma_{12} & \sigma_{13} \\ \sigma_{12} & \sigma_{22} & \sigma_{23} \\ \sigma_{13} & \sigma_{23} & \sigma_{33} \end{pmatrix} \tag{9}$$

$$\begin{aligned} W_\alpha^{el} = &-\tfrac{3}{2}\lambda_{100}\left[\sigma_{11}(\gamma_1^2 - \tfrac{1}{3}) + \sigma_{22}(\gamma_2^2 - \tfrac{1}{3}) + \sigma_{33}(\gamma_3^2 - \tfrac{1}{3})\right] \\ &-3\,\lambda_{111}\left(\sigma_{12}\,\gamma_1\,\gamma_2 + \sigma_{13}\,\gamma_1\,\gamma_3 + \sigma_{23}\,\gamma_2\,\gamma_3\right). \end{aligned} \tag{10}$$

It has to be emphasized that the condition on the magneto-crystalline energy ($W^K = \text{const.}$) supposes that no magnetization rotation occurs. In particular, it means that the level of stress is not high enough to generate magnetization rotation in the domains. This condition can be expressed as $|\boldsymbol{\sigma}_c : \boldsymbol{\varepsilon}_\alpha^\mu| \ll |K_1|$ in each domain.

The equilibrium configuration can be defined through the relative proportion of each domain family in the crystal. The volumetric fraction of a domain family is obtained using an explicit relation proposed by [7]:

$$f_\alpha = \frac{\exp(-A_s W_\alpha)}{\sum_\alpha \exp(-A_s W_\alpha)} = \frac{\exp(-A_s W_\alpha^{el})}{\sum_\alpha \exp(-A_s W_\alpha^{el})}. \tag{11}$$

A_s being a material parameter linked to the initial anhysteretic susceptibility χ_o and to the saturation magnetization M_s [5]:

$$A_s = \frac{3\chi_o}{\mu_o M_s^2}. \tag{12}$$

For further simplification, we introduce the quantity S:

$$S = \sum_\alpha \exp(-A_s W_\alpha^{el}). \tag{13}$$

An analytical model for the ΔE effect can then be derived from equation (11). Two cases are successively considered: material with $\langle 100\rangle$ easy magnetization axes (positive anisotropy constant) and material with $\langle 111\rangle$ easy magnetization axes (negative anisotropy constant).

3.1 Material with $\langle 100\rangle$ easy magnetization directions

3.1.1 Definition of variables

Six domain families have to be considered: they will be noted *abc*. The subscripts *abc* can take the value 100, $\overline{1}00$, 010, $0\overline{1}0$, 001 and $00\overline{1}$. The magnetization rotation mechanism being neglected, the magnetostriction strain tensor in each domain family is greatly simplified:

$$\boldsymbol{\varepsilon}_{abc}^\mu = \frac{1}{2}\lambda_{100}\begin{pmatrix} 3a^2 - 1 & 0 & 0 \\ 0 & 3b^2 - 1 & 0 \\ 0 & 0 & 3c^2 - 1 \end{pmatrix}. \tag{14}$$

The elastic energy for each domain family is then[4]:

$$W_{abc} = -\frac{1}{2}\lambda_{100}\left((3a^2-1)\sigma_{11} + (3b^2-1)\sigma_{22} + (3c^2-1)\sigma_{33}\right). \tag{15}$$

The quantity S is given by:

$$\begin{aligned} S = 2\Bigg[&\exp\left(A_s\lambda_{100}\left(\sigma_{11} - \frac{1}{2}(\sigma_{22} + \sigma_{33})\right)\right) \\ &+\exp\left(A_s\lambda_{100}\left(\sigma_{22} - \frac{1}{2}(\sigma_{11} + \sigma_{33})\right)\right) \\ &+\exp\left(A_s\lambda_{100}\left(\sigma_{33} - \frac{1}{2}(\sigma_{11} + \sigma_{22})\right)\right)\Bigg]. \end{aligned} \tag{16}$$

[4] It can be noticed that the shear terms of the stress tensor, expressed in the crystal coordinate system, do not appear in the definition of the elastic energy.

We deduce the associated volumetric fractions for each domain family:

$$\begin{cases} f_{100} = f_{\bar{1}00} = \dfrac{1}{S}\exp\left(A_s\lambda_{100}\left(\sigma_{11} - \frac{1}{2}\left(\sigma_{22}+\sigma_{33}\right)\right)\right) \\ f_{010} = f_{0\bar{1}0} = \dfrac{1}{S}\exp\left(A_s\lambda_{100}\left(\sigma_{22} - \frac{1}{2}\left(\sigma_{11}+\sigma_{33}\right)\right)\right) \\ f_{001} = f_{00\bar{1}} = \dfrac{1}{S}\exp\left(A_s\lambda_{100}\left(\sigma_{33} - \frac{1}{2}\left(\sigma_{11}+\sigma_{22}\right)\right)\right). \end{cases} \tag{17}$$

We can verify that, in accordance with experimental observation, no magnetization is created in the single crystal by application of a stress:

$$\overrightarrow{M_{\mathbf{c}}} = \sum_{\alpha} f_\alpha \overrightarrow{M_\alpha} = M_s \begin{vmatrix} f_{100} - f_{\bar{1}00} \\ f_{010} - f_{0\bar{1}0} \\ f_{001} - f_{00\bar{1}} \end{vmatrix} = \overrightarrow{0}. \tag{18}$$

But a magnetostriction strain $\boldsymbol{\varepsilon}_c^\mu$ is created by application of a stress:

$$\boldsymbol{\varepsilon}_c^\mu = \sum_{\alpha} f_\alpha \, \boldsymbol{\varepsilon}_\alpha^\mu \neq 0. \tag{19}$$

3.1.2 Uniaxial loadings

The case of a multiaxial applied stress can be first reduced to the simplified case of uniaxial loadings (tensile or compressive stress).

An uniaxial stress of amplitude σ along the [100] direction[5] leads to the strain ε_{100}^μ measured in the direction parallel to the applied stress[6]:

$$\varepsilon_{100}^\mu = \frac{\lambda_{100}\left[1 - \exp\left(-\frac{3}{2}A_s\lambda_{100}\,\sigma\right)\right]}{1 + 2\exp\left(-\frac{3}{2}A_s\lambda_{100}\,\sigma\right)}. \tag{20}$$

An uniaxial stress of amplitude σ along the [110] direction[7] leads to the strain ε_{110}^μ measured in the direction parallel to the applied stress:

$$\varepsilon_{110}^\mu = \frac{\lambda_{100}\left[1 - \exp\left(-\frac{3}{4}A_s\lambda_{100}\,\sigma\right)\right]}{2\left[2 + \exp\left(-\frac{3}{4}A_s\lambda_{100}\,\sigma\right)\right]}. \tag{21}$$

If an uniaxial stress of amplitude σ is applied along the [111] direction[8], we get:

$$f_{100} = f_{\bar{1}00} = f_{010} = f_{0\bar{1}0} = f_{001} = f_{00\bar{1}} = \frac{1}{6} \tag{22}$$

so that:

$$\boldsymbol{\varepsilon}_{111}^\mu = 0. \tag{23}$$

These results are plotted in Figure 3 in the case of iron for which $\lambda_{100} = 21 \times 10^{-6}$ [8]. The value for A_s is $5 \times 10^{-3}\,\mathrm{m^3\,J^{-1}}$.

[5] $\sigma_{ij} = 0$ except $\sigma_{11} = \sigma$.

[6] If ε_n^μ is the projection of the tensor $\boldsymbol{\varepsilon}^\mu$ in the direction $\boldsymbol{n}$, we have: $\varepsilon_n^\mu = {}^t\boldsymbol{n}\,\boldsymbol{\varepsilon}^\mu\,\boldsymbol{n}$.

[7] $\sigma_{ij} = 0$ except $\sigma_{11} = \sigma_{22} = \sigma_{12} = \frac{1}{2}\sigma$.

[8] $\sigma_{ij} = \frac{1}{3}\sigma$.

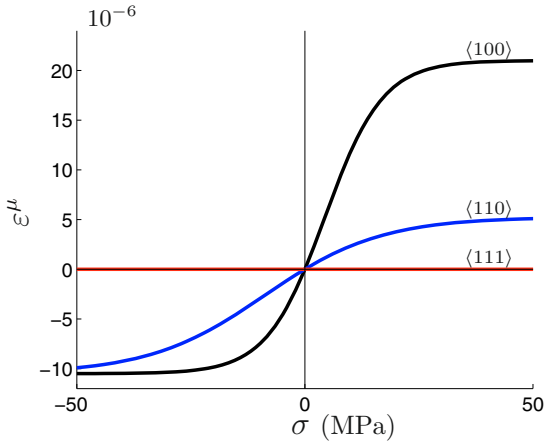

Fig. 3. (Color online) ΔE effect in the case of iron single crystal.

We can notice the dissymmetry between the tension and compression behaviors, visible for example in the values of the strain when – mechanical – saturation is reached:

$$\begin{cases} \lim_{(\sigma\to+\infty)} \varepsilon_{100}^\mu = \lambda_{100} \\ \lim_{(\sigma\to-\infty)} \varepsilon_{100}^\mu = -\dfrac{1}{2}\lambda_{100} \end{cases} \tag{24}$$

$$\begin{cases} \lim_{(\sigma\to+\infty)} \varepsilon_{110}^\mu = \dfrac{1}{4}\lambda_{100} \\ \lim_{(\sigma\to-\infty)} \varepsilon_{110}^\mu = -\dfrac{1}{2}\lambda_{100}. \end{cases} \tag{25}$$

3.1.3 Multiaxial loadings

More general and more complicated mechanical loadings can also be considered. We can study the particular cases of equi-bitension and hydrostatic pressure and compare them to uniaxial stress.

For example, under the hypotheses made, the magnetostriction strain in a ⟨100⟩ direction is defined, for any stress state, as:

$$\begin{aligned} \varepsilon_{100}^\mu &= \lambda_{100}\left(2f_{100} - f_{010} - f_{001}\right) \\ &= \frac{\lambda_{100}}{S}\left[2\exp\left(A_s\lambda_{100}\left(\sigma_{11} - \frac{1}{2}\left(\sigma_{22}+\sigma_{33}\right)\right)\right)\right. \\ &\quad -\exp\left(A_s\lambda_{100}\left(\sigma_{22} - \frac{1}{2}\left(\sigma_{11}+\sigma_{33}\right)\right)\right) \\ &\quad \left.-\exp\left(A_s\lambda_{100}\left(\sigma_{33} - \frac{1}{2}\left(\sigma_{11}+\sigma_{22}\right)\right)\right)\right]. \end{aligned} \tag{26}$$

The magnetostriction strain in a ⟨111⟩ direction is defined, for any stress state, as:

$$\varepsilon_{111}^\mu = 0. \tag{27}$$

Figure 4 shows the response of a single crystal under uniaxial[9], equibiaxial[10] and hydrostatic[11] loading along ⟨100⟩ directions.

We observe that a hydrostatic stress state has no effect on the magnetostriction strain.

[9] $\sigma_{ij} = 0$ except $\sigma_{11} = \sigma$.

[10] $\sigma_{ij} = 0$ except $\sigma_{11} = \sigma_{22} = \sigma$.

[11] $\sigma_{ij} = 0$ except $\sigma_{11} = \sigma_{22} = \sigma_{33} = \sigma$.

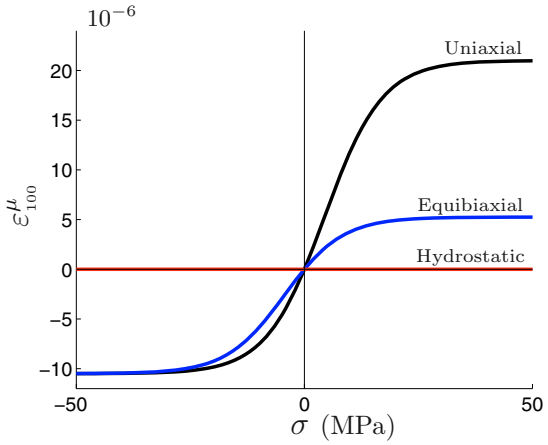

Fig. 4. (Color online) ΔE effect in the case of iron single crystal for a uniaxial, equibiaxial and hydrostatic loading along $\langle 100 \rangle$ directions.

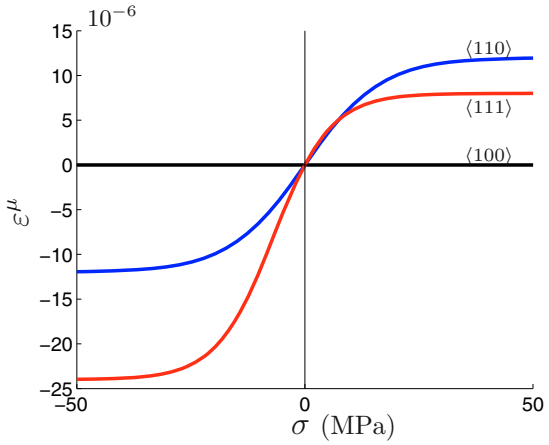

Fig. 5. (Color online) ΔE effect in the case of nickel single crystal.

3.2 Material with $\langle 111 \rangle$ easy magnetization directions

3.2.1 Definition of variables

In that case, eight domain families have to be considered: they will be noted *abc*. The subscripts *abc* take the values 111, $\overline{1}\overline{1}\overline{1}$, $\overline{1}11$, $1\overline{1}1$, $11\overline{1}$, $\overline{1}1\overline{1}$, $1\overline{1}\overline{1}$ and $\overline{1}\overline{1}1$. The magnetization rotation mechanism being neglected, the magnetostriction strain tensor in each domain family is also greatly simplified:

$$\boldsymbol{\varepsilon}^{\mu}_{abc} = \frac{1}{2}\lambda_{111}\begin{pmatrix} 0 & ab & ac \\ ab & 0 & bc \\ ac & bc & 0 \end{pmatrix}. \tag{28}$$

The elastic energy for each domain family is then[12]:

$$W_{abc} = -\lambda_{111}\,(ab\,\sigma_{12} + ac\,\sigma_{13} + bc\,\sigma_{23}). \tag{29}$$

The quantity S is given by:

$$\begin{aligned} S = 2\,[&\exp\left(A_s\lambda_{111}\,(\sigma_{12}+\sigma_{13}+\sigma_{23})\right) \\ &+\exp\left(A_s\lambda_{111}\,(-\sigma_{12}-\sigma_{13}+\sigma_{23})\right) \\ &+\exp\left(A_s\lambda_{111}\,(-\sigma_{12}+\sigma_{13}-\sigma_{23})\right) \\ &+\exp\left(A_s\lambda_{111}\,(\sigma_{12}-\sigma_{13}-\sigma_{23})\right)]\,. \end{aligned} \tag{30}$$

We deduce the associated volumetric fractions for each domain family:

$$\begin{cases} f_{111} = f_{\overline{1}\overline{1}\overline{1}} = \dfrac{1}{S}\exp\left(A_s\lambda_{111}\,(\sigma_{12}+\sigma_{13}+\sigma_{23})\right) \\ f_{\overline{1}11} = f_{\overline{1}\overline{1}1} = \dfrac{1}{S}\exp\left(A_s\lambda_{111}\,(-\sigma_{12}-\sigma_{13}+\sigma_{23})\right) \\ f_{1\overline{1}1} = f_{\overline{1}1\overline{1}} = \dfrac{1}{S}\exp\left(A_s\lambda_{111}\,(-\sigma_{12}+\sigma_{13}-\sigma_{23})\right) \\ f_{11\overline{1}} = f_{\overline{1}\overline{1}1} = \dfrac{1}{S}\exp\left(A_s\lambda_{111}\,(\sigma_{12}-\sigma_{13}-\sigma_{23})\right). \end{cases} \tag{31}$$

[12] It can be noticed that the diagonal terms of the stress tensor, expressed in the crystal coordinate system, do not appear in the definition of the elastic energy.

Here again, we verify that no magnetization can be created by application of a stress, but a magnetostriction strain $\boldsymbol{\varepsilon}^{\mu}_{c}$ appears:

$$\boldsymbol{\varepsilon}^{\mu}_{c} = \sum_{\alpha} f_{\alpha}\,\boldsymbol{\varepsilon}^{\mu}_{\alpha} \neq 0. \tag{32}$$

3.2.2 Uniaxial loadings

We study first the uniaxial case. An uniaxial stress of amplitude σ along the [111] direction leads to the strain ε^{μ}_{111} measured in the direction parallel to the applied stress:

$$\varepsilon^{\mu}_{111} = \frac{\lambda_{111}\,\left[1-\exp\left(-\frac{4}{3}A_s\lambda_{111}\,\sigma\right)\right]}{1+3\exp\left(-\frac{4}{3}A_s\lambda_{111}\,\sigma\right)}. \tag{33}$$

An uniaxial stress of amplitude σ along the [110] direction leads to the strain ε^{μ}_{110} measured in the direction parallel to the applied stress:

$$\varepsilon^{\mu}_{110} = \frac{1}{2}\lambda_{111}\tanh\left(\frac{1}{2}A_s\lambda_{111}\,\sigma\right). \tag{34}$$

If an uniaxial stress of amplitude σ is applied along the [100] direction, we get:

$$\begin{aligned} f_{111} &= f_{\overline{1}\overline{1}\overline{1}} = f_{\overline{1}11} = f_{1\overline{1}\overline{1}} \\ &= f_{1\overline{1}1} = f_{\overline{1}1\overline{1}} = f_{11\overline{1}} = f_{\overline{1}\overline{1}1} = \tfrac{1}{8} \end{aligned} \tag{35}$$

so that:

$$\boldsymbol{\varepsilon}^{\mu}_{100} = 0. \tag{36}$$

These results are reported in Figure 5 in the case of nickel for which $\lambda_{111} = -24\times10^{-6}$ [8]. The value for A_s is $5\times10^{-3}\,\mathrm{m^3\,J^{-1}}$ (the same than for the iron single crystal).

The dissymmetry between the tension and compression behaviors can also be noticed:

$$\begin{cases} \lim_{(\sigma\to+\infty)}\,\varepsilon^{\mu}_{111} = -\dfrac{1}{3}\lambda_{111} \\ \lim_{(\sigma\to-\infty)}\,\varepsilon^{\mu}_{111} = \lambda_{111} \end{cases} \tag{37}$$

$$\begin{cases} \lim_{(\sigma\to+\infty)} \varepsilon^{\mu}_{110} = -\dfrac{1}{2}\lambda_{111} \\ \lim_{(\sigma\to-\infty)} \varepsilon^{\mu}_{110} = \dfrac{1}{2}\lambda_{111}. \end{cases} \tag{38}$$

3.2.3 Multiaxial loadings

As previously said, the proposed modeling allows to consider more general and more complicated loadings.

The magnetostriction strain in a $\langle 100\rangle$ direction is defined, for any stress state, as:

$$\varepsilon^{\mu}_{100} = 0. \tag{39}$$

The magnetostriction strain in a $\langle 111\rangle$ direction is defined, for any stress state, as:

$$\begin{aligned} \varepsilon^{\mu}_{111} &= \frac{2}{3}\lambda_{111}\left(3f_{111} - f_{\overline{1}11} - f_{1\overline{1}1} - f_{11\overline{1}}\right) \\ &= \frac{2\lambda_{111}}{3S}\left[3\exp\left(A_s\lambda_{111}\left(\sigma_{12}+\sigma_{13}+\sigma_{23}\right)\right)\right. \\ &\quad -\exp\left(A_s\lambda_{111}\left(-\sigma_{12}-\sigma_{13}+\sigma_{23}\right)\right) \\ &\quad -\exp\left(A_s\lambda_{111}\left(-\sigma_{12}+\sigma_{13}-\sigma_{23}\right)\right) \\ &\quad \left.-\exp\left(A_s\lambda_{111}\left(\sigma_{12}-\sigma_{13}-\sigma_{23}\right)\right)\right]. \end{aligned} \tag{40}$$

We developed a fully analytical model of the effect of – uniaxial and multiaxial – stress on the magnetostriction strain of cubic single crystals. This modeling allows a description of the ΔE effect consistent with the independence of the elastic properties of materials on their magnetization. The same principles can be applied to the prediction of the behavior of polycrystals.

4 Extension to the behavior of polycrystals

The magnetostrictive behavior of a polycrystal is supposed, as a first approximation, to be isotropic. The contrast of behavior along different directions, exhibited for example in Figure 3 for the single crystal should not appear. The isotropic polycrystal can be seen as an aggregate of single crystals with random orientation. It can be defined as a single crystal for which all directions would be easy directions. In one domain of such a single crystal, the magnetostriction strain tensor can be written[13] (in the appropriate coordinate system):

$$\boldsymbol{\varepsilon}^{\mu}_{m} = \frac{1}{2}\lambda_{\mathrm{m}}\begin{pmatrix} 2 & 0 & 0 \\ 0 & -1 & 0 \\ 0 & 0 & -1 \end{pmatrix}, \tag{41}$$

λ_{m} denotes, for the polycrystal, the maximum magnetostriction strain that can be reached during a mechanical loading. The definition of its value requires a discussion.

[13] In accordance with the usual isochoric hypothesis for the magnetostriction strain [2].

4.1 Definition of λ_{m}

λ_{m} is the value of the maximum magnetostriction strain. This parameter can be identified from experimental measurements on unstrained specimen, but it can also be defined from the value of the single crystal magnetostriction coefficient λ_{100} or λ_{111}. It is shown in [5] that the maximum magnetostriction strain λ_{m} of a polycrystal, in the case when no magnetization rotation occurs can be written in the form:

$$\begin{aligned} \lambda_{\mathrm{m}} &= \tfrac{2}{5}\lambda_{100}k^{\mathbf{a}} \quad \text{for materials with} \\ &\qquad \langle 100\rangle \text{ easy directions}, \\ \lambda_{\mathrm{m}} &= \tfrac{3}{5}\lambda_{111}k^{\mathbf{b}} \quad \text{for materials with} \\ &\qquad \langle 111\rangle \text{ easy directions}, \end{aligned} \tag{42}$$

where $k^{\mathbf{a}}$ and $k^{\mathbf{b}}$ depend on the elastic properties of the single crystal and on the hypotheses chosen for the description of the material. For instance, if we choose uniform stress (Reuss) hypotheses, we have $k^{\mathbf{a}} = k^{\mathbf{b}} = 1$, and if we choose uniform strain (Voigt) hypotheses, we have $k^{\mathbf{a}} = 5\mu_a/(2\mu_a + 3\mu_b)$ and $k^{\mathbf{b}} = 5\mu_b/(2\mu_a + 3\mu_b)$, μ_a and μ_b being the cubic shear modulus of the single crystal. For the sake of simplicity, we will chose $k^{\mathbf{a}} = k^{\mathbf{b}} = 1$ in further numerical applications.

4.2 Multiaxial stress state

A general stress tensor is considered, with 6 independent components (see Eq. (9)). We choose to work in the principal coordinate system for the stress: in that particular framework, the stress tensor is diagonal and its components are called the principal stresses:

$$\boldsymbol{\sigma} = \begin{pmatrix} \sigma_{\mathrm{I}} & 0 & 0 \\ 0 & \sigma_{\mathrm{II}} & 0 \\ 0 & 0 & \sigma_{\mathrm{III}} \end{pmatrix}. \tag{43}$$

The definition of the magnetostriction strain of the polycrystal then follows the same strategy used for single crystals. Since a finite number of easy magnetization directions has been replaced by an infinite number, the symbol sum has to be replaced by an integral over the possible directions α.

The transformation matrix from the domain coordinate system to the principal coordinate system is noted $\boldsymbol{P}$ and defined by equation (44) where θ varies from 0 to 2π and φ from 0 to π

$$\boldsymbol{P} = \begin{pmatrix} \cos\theta\,\sin\varphi & \sin\theta & \cos\theta\cos\varphi \\ \sin\theta\,\sin\varphi & -\cos\theta & \sin\theta\sin\varphi \\ \cos\varphi & 0 & -\sin\varphi \end{pmatrix}. \tag{44}$$

The magnetostriction strain in a domain $\alpha(\theta, \varphi)$ can be expressed in the principal coordinate system according to equation (45)

$$\boldsymbol{\varepsilon}^{\mu}_{p} = {}^{t}\boldsymbol{P}\,\boldsymbol{\varepsilon}^{\mu}_{m}\,\boldsymbol{P}. \tag{45}$$

In such conditions:

$$\begin{cases} \varepsilon^{\mu}_{p11} = \dfrac{\lambda_{\mathrm{m}}}{2}\,(3\,\cos^2\theta\,\sin^2\varphi - 1) \\ \varepsilon^{\mu}_{p22} = \dfrac{\lambda_{\mathrm{m}}}{2}\,(3\,\sin^2\theta\,\sin^2\varphi - 1) \\ \varepsilon^{\mu}_{p33} = \dfrac{\lambda_{\mathrm{m}}}{2}\,(3\,\cos^2\varphi - 1) \\ \varepsilon^{\mu}_{p12} = \varepsilon^{\mu}_{21} = \dfrac{3\,\lambda_{\mathrm{m}}}{2}\,\cos\theta\,\sin\theta\,\sin^2\varphi \\ \varepsilon^{\mu}_{p13} = \varepsilon^{\mu}_{31} = \dfrac{3\,\lambda_{\mathrm{m}}}{2}\,\cos\theta\,\cos\varphi\,\sin\varphi \\ \varepsilon^{\mu}_{p23} = \varepsilon^{\mu}_{32} = \dfrac{3\,\lambda_{\mathrm{m}}}{2}\,\sin\theta\,\cos\varphi\,\sin\varphi. \end{cases} \tag{46}$$

The elastic energy in a domain α, defined by equation (47), can be developed according to equation (48).

$$W^{el}_{\alpha} = -\boldsymbol{\sigma} : \boldsymbol{\varepsilon}^{\mu}_{p} \tag{47}$$

$$\begin{aligned} W^{el}_{\alpha} = -\tfrac{1}{2}\lambda_{\mathrm{m}}\big[&\sigma_{\mathrm{I}}\,(3\,\cos^2\theta\,\sin^2\varphi - 1) \\ &+\sigma_{\mathrm{II}}\,(3\,\sin^2\theta\,\sin^2\varphi - 1) \\ &+\sigma_{\mathrm{III}}\,(3\,\cos^2\varphi - 1)\big]\,. \end{aligned} \tag{48}$$

Parameter S of equation (13) is now defined by equation (49)

$$S = \int_0^{2\pi}\!\!\int_0^{\pi} \exp\left(-A_s\,W^{el}_{\alpha}\right)\ \sin\varphi\,d\varphi\,d\theta. \tag{49}$$

The magnetostrictive response $\boldsymbol{E}^{\mu}$ of the polycrystal can be defined in a similar way to the one obtained in a direction $\langle 100\rangle$ of a single crystal with $\langle 100\rangle$ easy magnetization directions (since all directions are easy axes)

$$\boldsymbol{E}^{\mu} = \int_{\alpha} f_{\alpha}\,\boldsymbol{\varepsilon}^{\mu}_{p}\,d\alpha \tag{50}$$

with:

$$f_{\alpha} = \frac{1}{S}\exp\left(-A_s\,W^{el}_{\alpha}\right). \tag{51}$$

The magnetostriction strain tensor components, defined in the principal coordinate system, are then written:

$$E^{\mu}_{ij} = \frac{1}{S}\int_0^{2\pi}\!\!\int_0^{\pi} \varepsilon^{\mu}_{pij}\exp\left(-A_s\,W^{el}_{\alpha}\right)\ \sin\varphi\,d\varphi\,d\theta. \tag{52}$$

In accordance with experimental observation, the predicted magnetostriction strain is isochoric:

$$E^{\mu}_{11} + E^{\mu}_{22} + E^{\mu}_{33} = 0. \tag{53}$$

Moreover, we observe that the principal coordinate system for the magnetostriction strain tensor is the principal coordinate system for the stress tensor, so that:

$$\boldsymbol{E}^{\mu} = \begin{pmatrix} E^{\mu}_{11} & 0 & 0 \\ 0 & E^{\mu}_{22} & 0 \\ 0 & 0 & E^{\mu}_{33} \end{pmatrix} = \begin{pmatrix} E^{\mu}_{\mathrm{I}} & 0 & 0 \\ 0 & E^{\mu}_{\mathrm{II}} & 0 \\ 0 & 0 & E^{\mu}_{\mathrm{III}} \end{pmatrix}. \tag{54}$$

4.3 Uniaxial tension-compression

The case of uniaxial tension-compression[14] of amplitude σ brings significant simplifications. The elastic energy (Eq. (48)) reduces to:

$$W^{el}_{\alpha} = -\frac{1}{2}\lambda_{\mathrm{m}}\sigma\left(3\,\cos^2\varphi - 1\right). \tag{55}$$

Parameter S (Eq. (49)) is re-written:

$$S = 2\pi\,\mathrm{e}^{\left(-\frac{1}{2}A_s\lambda_{\mathrm{m}}\sigma\right)}\int_0^{\pi}\exp\left(\frac{3}{2}A_s\lambda_{\mathrm{m}}\sigma\cos^2\varphi\right)\,\sin\varphi\,d\varphi. \tag{56}$$

The magnetostriction strain in the direction parallel to the applied stress is then defined by equation (57)

$$E^{\mu}_{\mathrm{III}} = \frac{\pi\lambda_{\mathrm{m}}}{S}\exp\left(-\frac{1}{2}A_s\lambda_{\mathrm{m}}\sigma\right)\,I_1 \tag{57}$$

with:

$$I_1 = \int_0^{\pi}(3\,\cos^2\varphi - 1)\exp\left(\frac{3}{2}A_s\lambda_{\mathrm{m}}\sigma\cos^2\varphi\right)\,\sin\varphi\,d\varphi. \tag{58}$$

The calculation of the other terms of the tensor allows to verify the following expression for the magnetostriction strain tensor:

$$\boldsymbol{E}^{\mu} = \frac{\pi\,\lambda_{\mathrm{m}}\,I_1}{2\,S}\exp\left(\frac{1}{2}A_s\lambda_{\mathrm{m}}\sigma\right)\begin{pmatrix} -1 & 0 & 0 \\ 0 & -1 & 0 \\ 0 & 0 & 2 \end{pmatrix}. \tag{59}$$

5 Experimental characterization of ΔE effect

The measurement of ΔE effect usually consists in the evaluation of the stress-strain response of a demagnetized specimen (Fig. 1) thanks to a tensile-compressive machine. The ε^{μ} component of the total deformation is then extracted according to equation (2). This procedure is nevertheless very difficult to apply since amplitude of magnetostriction is most of the time much lower than the total deformation ε. Polycrystalline iron is a classical example: the amplitude of longitudinal magnetostriction is about 10^{-5}; considering a Young's modulus of about 200 GPa, a 2 MPa tensile stress produces the same elastic amplitude of deformation than magnetostriction. When stress overcomes 20 MPa, the deformation of magnetostriction only accounts for 10% of the total deformation. This way of measurement is consequently not accurate. Other methods can be used [9]. An alternative procedure, based on the hypothesis of magnetic saturation of the magnetostriction, is proposed in the next section.

5.1 Principle

The procedure is based on anhysteretic magnetostriction measurements under different levels of applied stress i.e.

[14] For example $\sigma_{\mathrm{I}} = \sigma_{\mathrm{II}} = 0$ and $\sigma_{\mathrm{III}} = \sigma$.

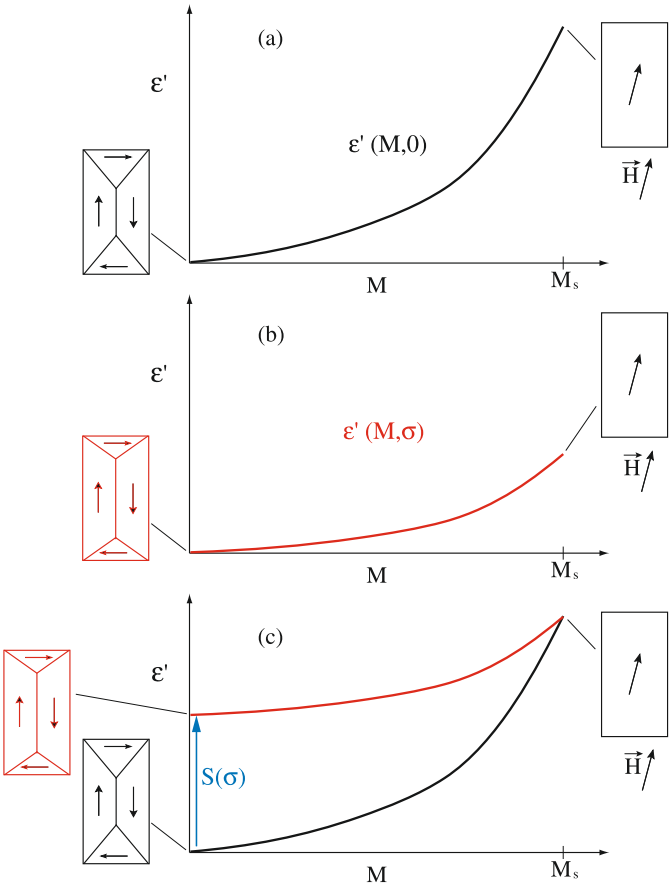

Fig. 6. (Color online) Schematic view of the measured deformation ε' and associated domain structure; (a) zero stress; (b) with σ applied stress; (c) shift of the σ applied stress curve to get the same saturation value.

$\varepsilon^{\mu}(M,\sigma)$ with σ constant. Accurate measurements require first to proceed to an efficient demagnetization under stress. This step leads to an initial deformation ε_i (Eq. (60)) that is practically not possible to measure.

$$\varepsilon_i(0,\sigma) = \varepsilon^{el}(\sigma) + \varepsilon^{\mu}(0,\sigma). \tag{60}$$

The deformation is then arbitrarily put to zero. Next step is to proceed to the anhysteretic magnetostriction measurement. Measurement is now corresponding to ε' given by equation (61):

$$\begin{aligned}\varepsilon'(M,\sigma) &= \varepsilon(M,\sigma) - \varepsilon_i(0,\sigma)\\ &= \varepsilon^{\mu}(M,\sigma) - \varepsilon^{\mu}(0,\sigma).\end{aligned} \tag{61}$$

The value of $\varepsilon'(M=0,\sigma)$ is artificially zero whatever the stress level. The extraction of magnetostriction behavior $\varepsilon^{\mu}(M,\sigma)$ requires consequently to evaluate $\varepsilon^{\mu}(0,\sigma)$.

Figure 6 gives a schematic view of $\varepsilon'(M,\sigma)$ for $\sigma = 0$ (a) and $\sigma \neq 0$ (b). A very simple 2D scheme of the domain configuration is associated. If we make the hypothesis that the magnetization reaches M_s at high magnetic field, the domain configurations and thus the values of magnetostriction are strictly identical whatever the stress level. The ultimate value $\varepsilon'(M_s,0) = \varepsilon^{\mu}(M_s,0)$ becomes a reference value that all the $\varepsilon'(M,\sigma)$ curves must reach. We finally proceed to a shift $S(\sigma)$ of the $\varepsilon'(M,\sigma)$ curves (Fig. 6c). $S(\sigma)$ is intrinsically corresponding to the magnetostriction at zero applied field i.e. $S(\sigma) = \varepsilon^{\mu}(0,\sigma)$, that is a direct observation of the ΔE effect. We note $S(\sigma) = \varepsilon^{\mu}(\sigma)$. Considering several stress levels σ, Figure 6c is consequently corresponding to the complete magnetostriction behavior $\varepsilon^{\mu}(M,\sigma)$[15].

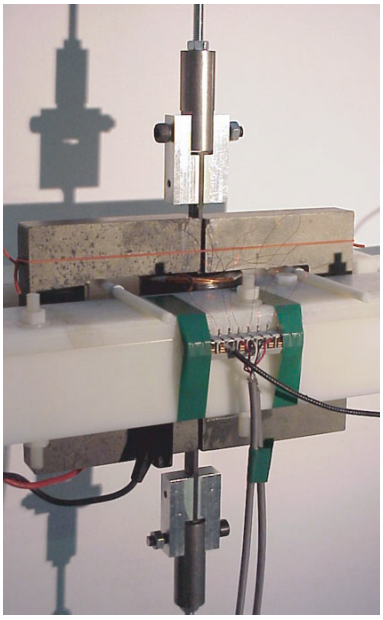

Fig. 7. (Color online) Apparatus for measurement of magnetostriction under applied stress – with articulated heads.

5.2 Experimental procedure

The benchmark for magneto-mechanical measurements is based on a non-standard experimental frame [10]. It is constituted of two face-to-face positioned ferrimagnetic U-yokes (Fig. 7). Samples are placed between the two yokes. Their shape and length depend on the nature of the investigated material. In order to measure magnetostriction, samples have been instrumented with longitudinal and transverse strain gages. A half Wheatstone bridge configuration with temperature compensation has been chosen for strain measurement (low-pass second order Butterworth filtering). A primary winding is placed on the specimen. B-coil and H-coil ensure the measurement of magnetic quantities.

We restrict the experiment to reversible behavior with usual methods (so-called anhysteretic measurement).

[15] It is not rigorously "pure" magnetostriction because the parasitic elastic deformation due to the magnetic forces still remains (i.e. form effect). This deformation is sometimes of same order of magnitude and has the same dynamic (frequency, even function) than magnetostriction. A second correction procedure should be applied especially with sheet specimen. But, because $\varepsilon^{\mu}(\sigma)$ is corresponding to a zero magnetization level, the correction is not necessary for this figure.

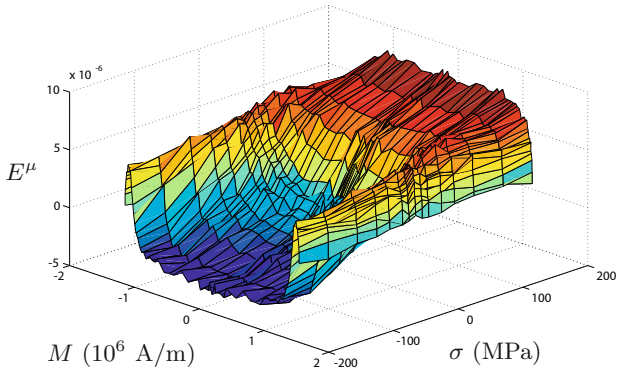

Fig. 8. (Color online) Influence of uniaxial stress on the anhysteretic longitudinal magnetostrictive behavior of pure iron [11].

The anhysteretic curves are measured point by point by applying a sinusoidal magnetic field of mean value H, and of exponentially decreasing amplitude.

Two solutions are possible to get uniaxial stress: the first solution is to suspend loads to the specimen, which is previously equipped with specific articulated heads (Fig. 7)[16]. This technique creates a pure uniaxial stress state and avoid vibrations, but compression is not possible; it is used for sheet format specimen (iron-silicon, iron-cobalt). The second solution is to use a hydraulic machine. This solution leads to noisy deformation measurements but enables compression. It is used for bulk materials (pure iron, Ni-Zn ferrite). The procedure detailed in Section 5.1 is finally applied.

Figure 8 gives an example of measurement carried out with the experimental set-up [11]. It shows the longitudinal magnetostrictive behavior of pure iron under tensile and compressive stress[17]. $\varepsilon^\mu(\sigma)$ is extracted from this measurement and plotted in Figure 9 for longitudinal and transverse directions.

Experimental results have been carried out with other materials: they are compared to the previsions of the model in the next section.

6 Comparison between experiments and modeling

The ΔE effect measurement has been performed on four different materials. Bulk specimens of pure iron and NiZn ferrite (composition $Ni_{0.48}Zn_{0.52}Fe_2O_4$), and sheet specimen of non-oriented 3%silicon-iron and 29%cobalt-iron alloys have been tested. The magnetostriction coefficients of the single crystals of these materials are reported in Table 1. The variables $k^{\mathbf{a}}$ and $k^{\mathbf{b}}$ (Eq. (42)) have been arbitrarily taken equal to 1, corresponding to uniform stress hypotheses. The data used for the modeling are given in Table 2.

[16] The maximal load is about 50 kg leading to a maximal stress from 16 MPa to 100 MPa depending on the section of the specimen.

[17] The specimen is a 10 mm diameter plain cylinder of iron; form effect is negligible and so not withdrawn to the results.

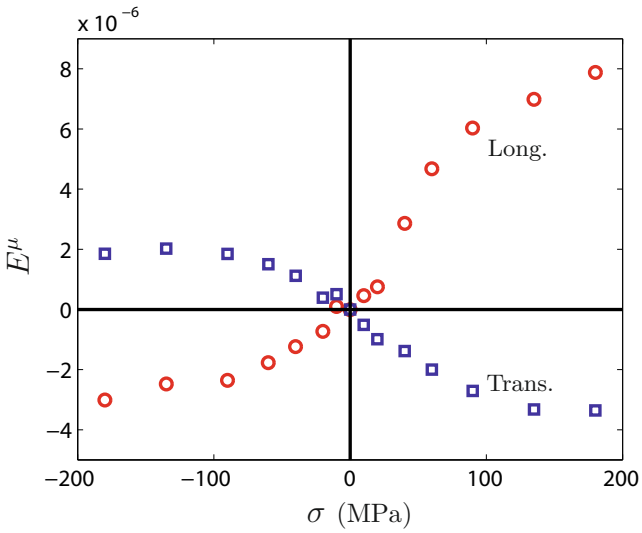

Fig. 9. (Color online) ΔE effect for pure iron – longitudinal and transverse behaviors.

Table 1. Magnetostriction constants of the materials used for experiments.

	λ_{100}	λ_{111}	K_1 (J m^{-3})	Ref.
Pure iron	21×10^{-6}	-21×10^{-6}	42 700	[6,8]
Ni-Zn ferrite	-26×10^{-6}	-5×10^{-6}	−1700	[12]
FeSi alloy	25×10^{-6}	-5×10^{-6}	38 000	[6,8]
FeCo alloy	100×10^{-6}	10×10^{-6}	35 000	[13]

Table 2. Modeling parameters.

	A_s (m^3/J)	λ_m
Pure iron	5×10^{-3}	8.4×10^{-6}
Ni-Zn ferrite	3×10^{-2}	-3.0×10^{-6}
FeSi alloy	3×10^{-2}	10×10^{-6}
FeCo alloy	5×10^{-3}	40×10^{-6}

6.1 Bulk specimens

The results for pure iron and Ni-Zn bulk specimens are respectively presented in Figures 10 and 11. Figure 10 exhibits a very good agreement between modeling and experimental results. Some significant discrepancies are observed for Ni-Zn ferrite. A higher value for λ_m would be necessary in the modeling to get a better agreement. Considering the elastic constants of the single crystal [12], another mechanical hypothesis than uniform stress state would not lead to a significant change of λ_m. The relatively low value of K_1 explains these discrepancies: indeed for such a low magnetocrystalline anisotropy, the hypothesis of no magnetization rotation under stress is not verified. The maximum value for the magnetostriction strain cannot be defined as simply as in equation (42). This results points out a limitation of the proposed approach. In such a case, where the behavior results from the combinaison

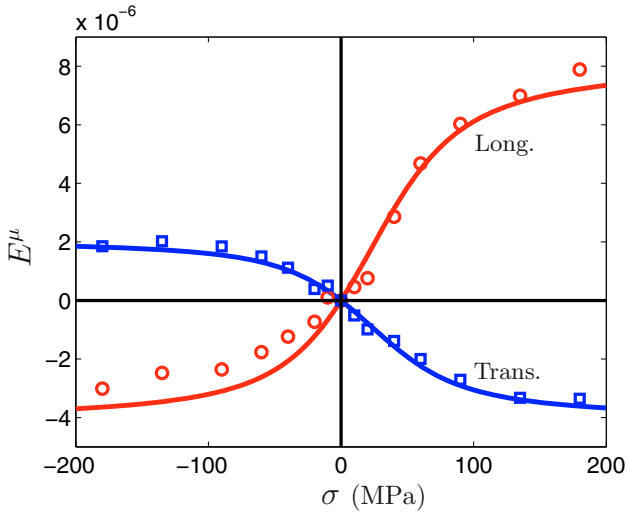

Fig. 10. (Color online) ΔE effect for pure iron: longitudinal and transverse magnetostriction strain as a function of the applied stress σ, modeling (line) and experimental results.

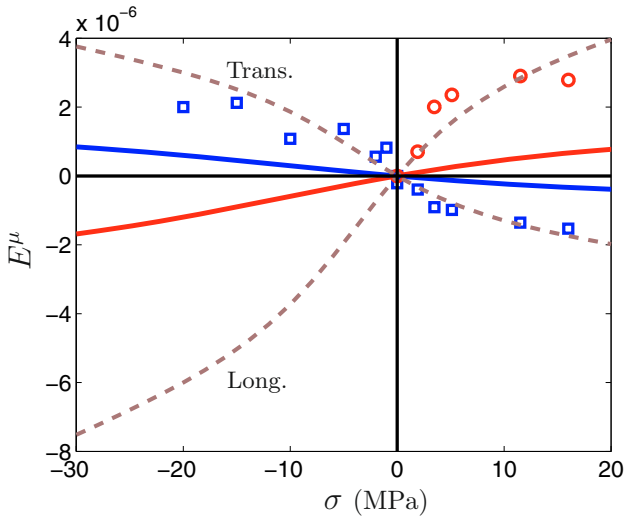

Fig. 11. (Color online) ΔE effect for Ni-Zn ferrite: longitudinal and transverse magnetostriction strain as a function of the applied stress σ, modeling (line) and experimental results. Dashed lines: results obtained with a full multiscale model [12].

of domain wall motion and magnetization rotation mechanisms, the full multiscale model [5] should be used. The corresponding results (presented in reference [12]) have been added in Figure 11.

6.2 Sheet specimens

The results for iron-silicon and iron-cobalt sheet specimens[18] are respectively presented in Figures 12 and 13.

The agreement between modeling (plain lines) and experimental (points) results is good considering the longitudinal direction, but the comparison is not satisfactory in the transverse direction. The explanation of these discrepancies may be found in the initial distribution of the magnetic domains in the material. Indeed the model is designed for bulk materials so that the initial distribution of the domains is assumed to be random into a uniform distribution (every domain directions have the same probability of existence). As a consequence, the behavior

[18] In both cases, the experimental data have been collected with a tensile stress applied in the direction TD perpendicular to the rolling direction of the sheet.

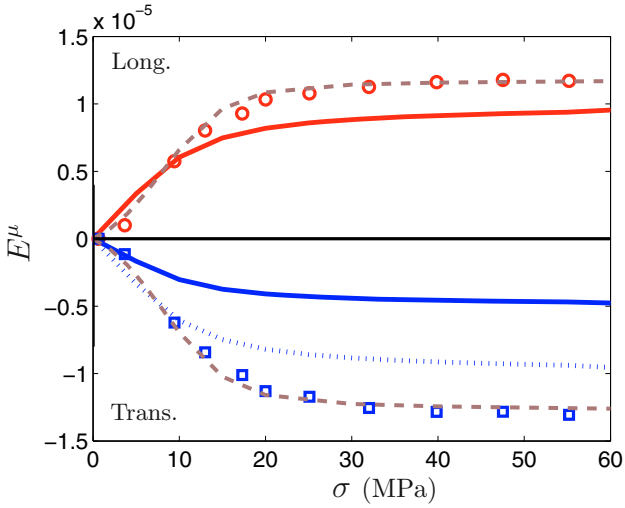

Fig. 12. (Color online) ΔE effect for an iron-silicon steel: longitudinal and transverse magnetostriction strain as a function of the applied stress σ, modeling (line) and experimental (points) results. Plain line for isotropic strain and dot line (transverse direction) for configuration energy effect. Dashed lines: results obtained with a full multiscale model with configuration energy effect [5,15,16].

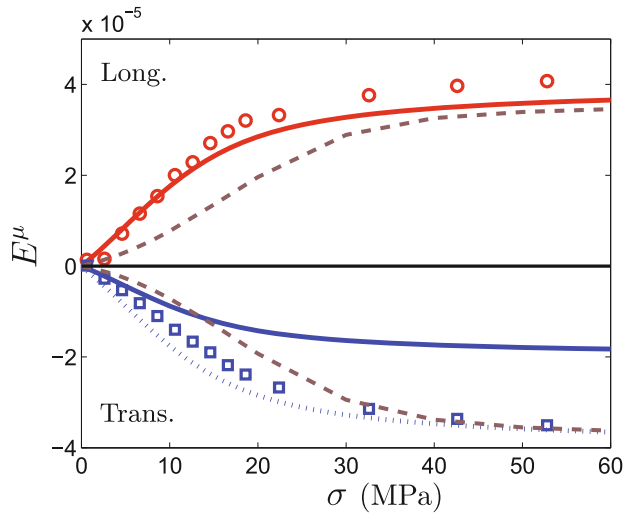

Fig. 13. (Color online) ΔE effect for an iron-cobalt alloy: longitudinal and transverse magnetostriction strain as a function of the applied stress σ, modeling (line) and experimental (points) results. Plain line for isotropic strain and dot line (transverse direction) for configuration energy effect. Dashed lines: results obtained with a full multiscale model with configuration energy effect [5,15,16].

is isotropic and the transverse magnetostriction is equivalent in any direction perpendicular to the longitudinal direction. Considering an isochoric strain, it comes:

$$E^{\mu}_{\text{Trans}} = -\frac{1}{2} E^{\mu}_{\text{Long}}. \tag{62}$$

This hypothesis obviously does not apply to sheet specimen. For such shapes, demagnetizing phenomena lead to a non-uniform distribution of domains [14,15]. This initial configuration is such that the domains with magnetization along the rolling direction of the sheet are in higher proportion than the others[19]. As a consequence, the behavior is anisotropic. The simplifying hypotheses used do not apply. However, the ΔE effect can be predicted using the full – numerical – multiscale model [5]. The initial configuration is taken into account in the model using configuration energy [15,16]. This procedure has been applied to iron-silicon and iron-cobalt alloys. Results are plotted in Figures 12 and 13 (dashed lines) showing a better agreement with experimental results.

It appears that the magnetostriction strain in the direction perpendicular to the sheet is close to zero (for these materials). The transverse magnetostriction strain satisfies the relation (63).

$$E^{\mu}_{\text{Trans}} = -E^{\mu}_{\text{Long}}. \tag{63}$$

Using this result as an hypothesis for the analytical model, the agreement between experimental and model data (dot line in Fig. 13 and 12) becomes better.

7 Conclusion

A model for the ΔE effect in magnetic materials has been proposed. This model is based on the description of the physical mechanisms responsible for magneto-elastic couplings at the single crystal scale. The proposed analytical approach does not include magnetization rotation as a source of magnetostriction strain. It is limited to material exhibiting high magneto-crystalline constants. A specific procedure for the experimental characterization of the ΔE effect has been proposed. Modeling and experimental results have been compared for bulk and sheet polycrystalline specimen. The results on Ni-Zn ferrite have allowed to illustrate the limitations and conditions of use of the model. In the case of sheet samples, an initial domain configuration has to be accounted for. This model provides a simple tool to describe the effect of stress on the magnetostriction strain. It could be used in electrical engineering to improve the macroscopic models for magneto-elastic coupling, that often neglect the effect of stress on magnetostriction.

[19] This change (compared to the uniform distribution) depends on the material composition, on the crystallographic texture, on the dimensions and on the forming process of the sheet.

References

1. B.D. Cullity, *Introduction to magnetic Materials* (Addison-Wesley Publishing Company, 1972)
2. E. du Trémolet de Lacheisserie, *Magnetostriction – Theory and applications of magnetoelasticity* (CRC Press, 1993)
3. P.T. Squire, J. Mag. Magn. Mat. **87**, 299 (1990)
4. A. Hubert, R. Schäfer, *Magnetic domains* (Springer, 1998)
5. L. Daniel, O. Hubert, N. Buiron, R. Billardon, J. Mech. Phys. Sol. **56**, 3, 1018 (2008)
6. R.M. Bozorth, *Ferromagnetism* (Van Nostrand, 1951)
7. N. Buiron, L. Hirsinger, R. Billardon, J. Phys. IV France **9**, 139 (1999)
8. D.C. Jiles, *Introduction to Magnetism and Magnetic Materials* (Chapman & Hall, 1991)
9. P.T. Squire, J. Mag. Magn. Mat. **160**, 11 (1996)
10. O. Hubert, L. Daniel, R. Billardon, J. Mag. Magn. Mat. **254–255**, 352 (2003)
11. L. Lollioz, S. Pattofatto, O. Hubert, J. Electr. Eng. **57**, 8, 15 (2006)
12. L. Daniel, O. Hubert, B. Vieille, Int. J. Appl. Electromagn. Mech. **25**, 31 (2007)
13. P. Brissonneau, *Magnétisme et matériaux magnétiques* (Hermès, 1997)
14. L. Daniel, O. Hubert, R. Billardon, Int. J. Appl. Electromagn. Mech. **19**, 293 (2004)
15. O. Hubert, L. Daniel, J. Mag. Magn. Mat. **320**, 7, 1412 (2008)
16. O. Hubert, L. Daniel, J. Mag. Magn. Mat. **304**, 489 (2006)